Hassooni, Mohsin A.

Article

Theoretical analysis of charge flow rate at dye sensitized-semiconductor interfaces cell system

Energy Reports

Provided in Cooperation with:
Elsevier

Suggested Citation: Hassooni, Mohsin A. (2020) : Theoretical analysis of charge flow rate at dye sensitized-semiconductor interfaces cell system, Energy Reports, ISSN 2352-4847, Elsevier, Amsterdam, Vol. 6, Iss. 3, pp. 72-78, https://doi.org/10.1016/j.egyr.2019.10.020

This Version is available at:
https://hdl.handle.net/10419/243981

Available online at www.sciencedirect.com
ScienceDirect
Energy Reports 6 (2020) 72–78
www.elsevier.com/locate/egyr

Tmrees, EURACA, 04 to 06 September 2019, Athens, Greece

Theoretical analysis of charge flow rate at dye sensitized-semiconductor interfaces cell system

Mohsin A. Hassooni

Department of Physics, College of Education for pure science, Ibn Al-Haitham, University of Baghdad, Iraq

Received 19 September 2019; accepted 18 October 2019
Available online 26 October 2019

Abstract

The dynamics of charge flow at the interface of the Dye/Semiconductor cell has been investigated by a quantum transfer theory. At the interface between the N3 and Cresyl Violet CV dyes complex such as CdS and InAs semiconductor, the potential determines the flow charge transfer rate and indicates the efficiency of the devices. The flow charge rate at N3/CdS, N3/InAs, CV/CdS and CV/InAs were increased along with decreasing the energy of transition and increasing the coupling parameter. The potential at the interface also indicates the effect of the structure of the material on the flow charge rate in the dye-sensitized solar cells (DSSC) devices. The flow charge rate at DSSC system is polar dependent region. In this study, the flow charge rate was found to be highly compared to InAs by factor 10^2.

Peer-review under responsibility of the scientific committee of the Tmrees, EURACA, 2019.

Keywords: Flow charge; DSSC; Dye sensitized-semiconductor

1. Introduction

In the last few decades, demands for clean energy sources have been increased-drastically because of its necessity in the economic developments, social accommodation and human health. Since the beginning of the twentieth century, the use of clean energy in different areas of technology had been accelerated to reduce the tremendous increase in the emission of various gases such as (Co_2 and Co) and to moderate the climate of earth climate cooperation with the global warming effect [1]. Recently, the energy scenario tool had been changed leading to substantial increases in energies. In the central energy search sustainability was renewable energies. The society of nanotechnology and nanoscience can be assisted in solving several global energy problems [2]. One of the most essential devices that satisfy the growing demand for clean energies without any pollution is the photovoltaic (PV) device [3]. However, considerable efforts have been made to investigate and developed new sources of energy harvesting with sufficient conversion efficiencies for fuel generation by using solar energy [4]. In fact, the energy conversion process in the photovoltaic cell is mainly based on generating charge carriers from photons by absorption of light [5]. So far, dye sensitized solar cell or Gratzel cell has proved itself as an efficient clean energy source among

E-mail address: mohsin.a@ihcoedu.uobaghdad.edu.iq.

https://doi.org/10.1016/j.egyr.2019.10.020

Peer-review under responsibility of the scientific committee of the Tmrees, EURACA, 2019.

other sources [6]. The phenomenon of charge carrier's transfer within the molecules of a reliable interface system has been widely investigated and studied using different theoretical models and experimental techniques [7]. The dye-sensitized solar cells (DSSC) are semiconductor-based photovoltaic devices that directly convert solar radiation to electrical current. Basically, the semiconductor in the DSSC absorbs light by the sensitizer and the light separates the charge carrier to transport within the [8]. Understanding electron transportation processes in DSSC is very important for developing new technologies in the areas of molecular electronics and complex biological enzymes molecules [9]. In this study, a comprehensive investigation has been made to understanding the dynamics and study the flow charge transfer rate at the sensitized-semiconductor cell system.

2. Theory

According to the quantum theory, the phenomenon of charge carrier transport in the DSSC system can be described based on a simple model of donor–acceptor scenario. The electronic transfer current Λ_{CT} can be written according to golden rule [10]:

$$\Lambda_{CT} = \frac{2\pi}{\hbar}\mathfrak{M}_T{}^2\mathcal{G}_{S-D} \tag{1}$$

Here $\mathfrak{M}_T{}^2$ is the square coupling of electronic and $\mathcal{G}_{S-D}$ is Franck–Condon weight density. The $\mathcal{G}_{S-D}$ can be evaluated — by Perturbation methods of the potential barrier and is written as below [11].

$$\mathcal{G}_{S-D} = (\aleph\mathcal{T}_S^D)^{\frac{-1}{2}} exp - \frac{\pi\left(\mathfrak{O}_{Sem}^{Dye} + \mathcal{T}_S^D\right)^2}{\aleph\mathcal{T}_S^D} \tag{2}$$

where $\aleph = 4\pi k_B T$ is time dependent temperature value, k_B is Boltzmann constant and T is taken as room temperature, $\mathcal{T}_S^D$ is the transition energy, $\mathfrak{O}_{Sem}^{Dye}$ is the activation force energy. According to assumed continuum energy levels for both materials, the Eq. (1) has been rewritten as an integral equation with a distribution function of the electronic density of state $f_{(\epsilon)}$.

$$\Lambda_{CT} = \frac{2\pi}{\hbar}\int_{-\infty}^{\infty}|\mathfrak{M}_T|^2(\aleph\mathcal{T}_S^D)^{\frac{-1}{2}} exp - \frac{\pi\left(\mathfrak{O}_{Sem}^{Dye} + \mathcal{T}_S^D\right)^2}{\aleph\mathcal{T}_S^D} f_{(\epsilon)}d\epsilon \tag{3}$$

Here $f_{(\epsilon)}$ is the Fermi level of electronic density of state of the dye sensitized solar cell which can be written as [4].

$$f_{(\epsilon)} = \frac{1}{1 + e^{\frac{\epsilon-\epsilon_F}{k_B T}}} \tag{4}$$

The electrochemical potentials at Dye/Semiconductor interface that described by the exponential term in Eq. (3) can be written as.

$$\mathbb{U}_{Sem}^{Dye} \approx \frac{\pi\left(\mathfrak{O}_{Sem}^{Dye} + \mathcal{T}_S^D\right)^2}{\aleph\mathcal{T}_S^D} \tag{5}$$

By inserting Eqs. (5) and (4) in Eq. (3) and solving the resulted integral equation, the electronic which transfers current can be described by (6) [12].

$$\Lambda_{CT} \approx \frac{2\pi}{\hbar}(\aleph\mathcal{T}_S^D)^{\frac{-1}{2}}\left(\frac{NV^{Sem}}{\sum_0^\infty \rho\,(E)\,f_o\,(E)}\right)exp - \frac{\pi\left(\mathfrak{O}_{Sem}^{Dye} + \mathcal{T}_S^D\right)^2}{\aleph\mathcal{T}_S^D}|\mathfrak{M}_T|^2\left[\pi k_B T - \frac{(\pi k_B T)^2}{16\pi\mathcal{T}_S^D}\right] \tag{6}$$

On the other hand, the coefficient coupling for the steady state must be given as [13]:

$$\left\langle\left|\overline{\mathfrak{M}_T(0)}\right|^2\right\rangle = \frac{|\mathfrak{M}_T|^2}{\sum_0^\infty \rho\,(E)\,f_o\,(E)} \tag{7}$$

The rate of electronic transition current is relative to decay constant β_{CT}, and it is given by $\Lambda_{\mathbb{CT}}(\mathfrak{T}_S^D, |\mathbb{C}_T|^2, T) = \frac{1}{\beta_{CT}}\mathcal{F}_{CT}$ [14]. Then, by simplifying Eqs. (6) and (7).

$$\Lambda_{\mathbb{CT}}(\mathfrak{T}_S^D, |\mathfrak{M}_T|^2, T) \approx \frac{2\pi}{\hbar}\frac{NV^{Sem}}{\beta_{CT}}(\aleph\mathfrak{T}_S^D)^{\frac{-1}{2}}\left\langle\left|\overline{\mathfrak{M}_T(0)}\right|^2\right\rangle e^{-\frac{\pi\left(\mathfrak{O}_{Sem}^{Dye}+\mathfrak{T}_S^D\right)^2}{\aleph\mathfrak{T}_S^D}}\left[\pi k_B T - \frac{(\pi k_B T)^2}{16\pi\mathfrak{T}_S^D}\right] \tag{8}$$

The electronic transfer energies for DSSC system is [15].

$$\mathfrak{T}_S^D\ (\mathrm{eV}) = \frac{e^2}{8\pi\epsilon_\circ}\left[\frac{1}{R_{Dye}}\mathbb{f}\ (n_S, \epsilon_s) - \frac{1}{2d_{Dye-Sem}}\mathbb{f}(n_S, n_{Sem}, \epsilon_s, \epsilon_{Sem})\right] \tag{9}$$

where e is charge of the electron, $\epsilon_\circ$ is the permittivity of space. The solvent polarity function is given by:

$$\mathbb{f}\ (n_S, \epsilon_s) = \left(\frac{1}{{n_S}^2} - \frac{1}{\epsilon_s}\right) \tag{10}$$

where n_S and ϵ_s are the refractive index and dielectric constant for the solvent. While the polarity for dye–semiconductor system is:

$$\mathbb{f}(n_S, n_{Sem}, \epsilon_s, \epsilon_{Sem}) = \left(\frac{n_{Sem}^2 - {n_S}^2}{n_{Sem}^2 + {n_S}^2}\frac{1}{{n_S}^2} - \frac{\epsilon_{Sem}^2 - {\epsilon_S}^2}{\epsilon_{Sem}^2 + S}\frac{1}{{\epsilon_{Sem}}^2}\right) \tag{11}$$

where n_{Sem} and ϵ_{Sem} are the refractive index and dielectric constant for the semiconductor, R_{Dye} refers to the dye radius, and $d_{Dye-Sem}$ indicates the distance between the semiconductor and dye. The dye molecule radius can be estimated by [16]:

$$R_{Dye} = (\frac{3}{4\pi}\frac{M_{Dye}}{N\rho_{Dye}})^{\frac{1}{3}} \tag{12}$$

Here M_{Dye} indicates the molecular weight for dye, N and ρ_{Dye} are the Avogadro number, and dye density, respectively.

3. Results

Since the flow rate is a key aspect in understanding the dynamic of the electronic features and the efficiency of DSSC solar cell, it is important to study the parameters that may affect the flow rate, Fig. 1 shows a schematic diagram of the energy levels at DSSC interface.

The investigation of the charge flow rate $\Lambda_{\mathbb{CT}}$ at both CV/CdS and CV/InAs and N3/ CdS and N3/InAs dye-sensitized solar cells (DSSC) systems have been carried out based on the quantum theory by using the golden rule. MATLAB software was used to calculate the charge flow rate by solving Eq. (8) at room temperature. In order to calculate the flow rate of electrons, the energy of the transition $\mathfrak{T}_S^D$ and electronic coupling term between the dye and semiconductor states should be estimated. The energy of transition is the required energy for a system to align and reform prior to electron transition which can be calculated using Eq. (9). The radius of both dye and semiconductor were estimated from Eq. (12) by considering the density $\rho_{N3} = 1.261\ \frac{\mathrm{g}}{\mathrm{cm}^3}$, $\rho_{CV} = 1.92\ \frac{\mathrm{g}}{\mathrm{cm}^3}$, molecular weight $M_{N3} = 1187.08\ \frac{\mathrm{molecule}}{\mathrm{mole}}$, $M_{CV} = 361.74\ \frac{\mathrm{molecule}}{\mathrm{mole}}$, results are $r_{N3} = 6.5\ \mathring{A}$ and $r_{CV} = 4.21\ \mathring{A}$. By substituting the refractive index and dielectric constant of semiconductor and molecules solvent. The energy of transition for CV/CdS and CV/InAs and N3/ CdS and N3/InAs DSSC dye is estimated using Eq. (9) and the results are listed in Tables 1 to 3.

The activation force energy $\mathfrak{O}_{Sem}^{Dye}$ (eV) is also an important factor for electron transition from donor to the acceptor in all DSSC system. It can be calculated from the absorption spectrum in Fig. 2 and using the following equation $\mathfrak{O}_{Sem}^{Dye}\ (\mathrm{eV}) = h\upsilon - \mathfrak{T}_S^D$ by inserting the energy of transition from Tables 2 and 3. Estimated results for Cv/CdS, Cv/InAs and N3/CdS and N3/InAs are shown in Tables 4 and 5 respectively

The charge flow rate of electronic transition was calculated using Eq. (8) by considering the values of the average coupling coefficient and the transition energy for dye /semiconductor $\left\langle\left|\overline{\mathfrak{M}_T(0)}\right|^2\right\rangle$ taking from Tables 2 and 3 respectively. The lattice constant for both semiconductors were taken from Table 1, and the penetration factors are $\beta_{CT} = 1\mathring{A}^{-1}$. The results of charge flow rate for Cv/CdS, Cv/InAs and N3/CdS and N3/InAs are shown in Tables 6 and 7 respectively.

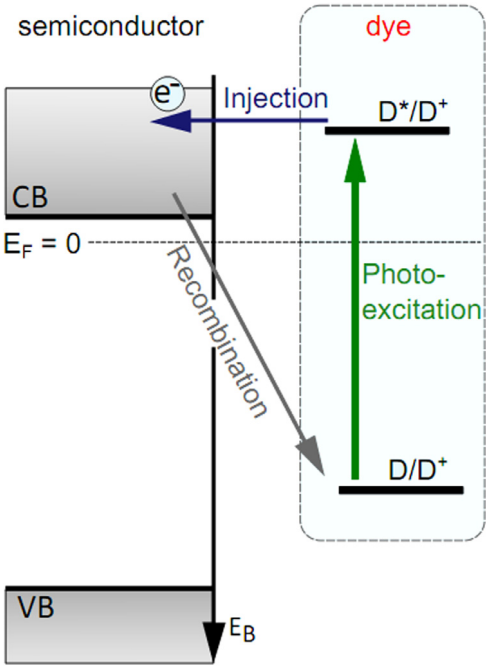

Fig. 1. Schematic of alignment energy levels at a DSSC interface.

Table 1. General characteristics of the used semiconductors.

Properties	CdS [17]	InAs [18]
Atomic weight (molecule/mole)	144.48	81.38
Crystal structure	Hexagonal cubic	Cubic
Density (g/cm^3)	4.826 g/cm^3	5.66
Refractive index	2.529	3.5
Dielectric constant	8.9	15
Radius calculated (Å)	2.281	2.367
Electron affinity	3.47 eV	4.9 (eV)

Table 2. Energy of transition for CV/CdS and CV/InAs DSSC at 1-propanol, Acetonitrile and Ethanol solvents.

Solvent	ϵ_{so} [19]	n [19]	$\mathfrak{T}_S^D$ (eV) for CV/CdS	$\mathfrak{T}_S^D$ (eV) for CV/InAs
1-propanol	20.33	1.3856	0.611811	0.5437945
Acetonitrile	37.5	1.3441	0.686607	0.616523
Ethanol	24.5	1.3614	0.646761	0.577585

Table 3. Energy of transition for N3/CdS and N3/InAs DCSC at 1-propanol, Acetonitrile and Ethanol solvents.

Solvent	ϵ_{so} [19]	n [19]	$\mathfrak{T}_S^D$ (eV) for N3/CdS	$\mathfrak{T}_S^D$ (eV) for N3/InAs
1-propanol	20.33	1.3856	0.387112	0.3398633
Acetonitrile	37.5	1.3441	0.434637	0.385951
Ethanol	24.5	1.3614	0.409217	0.361161

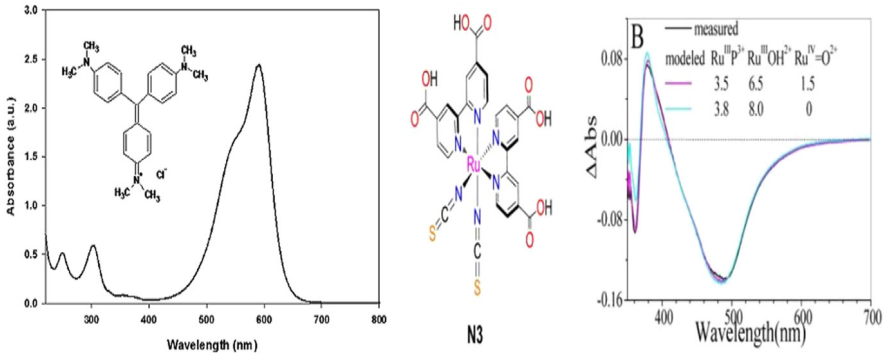

Fig. 2. (A) The chemical structure and the UV–Vis absorbance of CV and (B) The chemical structure and the UV–Vis absorbance of N3-dye.

Table 4. The activation driving energies for CV/CdS and CV/InAs DSSC at 1-Propanol, Acetontrile, and Ethanol solvents.

Wave length λ (nm)	Absorption energy (eV)	The active driving force energy $\mathfrak{O}_{Sem}^{Dye}$ (eV)					
		CV/CdS DCSC			CV/InAs DCSC		
		1-Propanol	Asetontrile	Ethanol	1-Propanol	Asetontrile	Ethanol
300	4.125	3.805	3.842	3.816	3.916	3.948	3.925
350	3.535	3.215	3.252	3.226	3.326	3.358	3.335
400	3.093	2.773	2.810	2.784	2.884	2.916	2.893
450	2.750	2.430	2.467	2.441	2.541	2.573	2.550
500	2.475	2.155	2.192	2.166	2.266	2.298	2.275
550	2.250	1.930	1.967	1.941	2.041	2.073	2.050
600	2.062	1.742	1.779	1.753	1.853	1.885	1.862
650	1.904	1.660	1.620	1.594	1.694	1.726	1.703
700	1.767	1.447	1.484	1.458	1.558	1.590	1.567

Table 5. The activation driving energies for N3/CdS and N3/InAs DSSC at 1-Propanol, Acetontrile, and Ethanol solvents.

Wave length λ (nm)	Absorption energy (eV)	The active driving force energy $\mathfrak{O}_{Sem}^{Dye}$ (eV)					
		N3/CdS DCSC			N3/InAs DCSC		
		1-Propanol	Asetontrile	Ethanol	1-Propanol	Asetontrile	Ethanol
400	3.093	2.705	2.658	2.683	2.754	2.708	2.732
450	2.750	2.363	2.316	2.341	2.411	2.365	2.389
500	2.475	2.088	2.041	2.066	2.136	2.090	2.114
550	2.250	1.863	1.816	1.841	1.911	1.865	1.889
600	2.062	1.675	1.628	1.653	1.723	1.677	1.701
650	1.904	1.517	1.470	1.495	1.565	1.519	1.543
700	1.767	1.380	1.333	1.358	1.4280	1.382	1.406

4. Discussion

The efficiency and the electrical properties of the DSSC system were affected by the charge flow rate of electronic transition $\Lambda_{\mathbb{CT}}(\mathfrak{T}_S^D, |\mathfrak{M}_T|^2, T)$ due to the transition energy $\mathfrak{T}_S^D$ (eV), and the active overlapping electronic coupling coefficient $\mathfrak{M}_T$ eV at a temperature T(K). Since the conducting band in both CdS and InAs semiconductors were assumed to be a continuous energy level as mentioned previously. Both CV and N3 DSSC dye molecule are bounding to these semiconductors. The charge flow rate has been evaluated according to transition energy $\left(\mathfrak{T}_S^D\right)$., that is energy must the system has to reform to begin the transition and the energy of overlapping the electronic energy state to coupling each other to continue transition due to interface. The unit cell volume and penetration

Table 6. The charge flow rate of electron transfer $\Lambda_{\mathbb{CT}}(\mathcal{T}_S^D, |\mathfrak{M}_T|^2, T)$.

Average coupling coefficient	The current of electron transfer $\Lambda_{\mathbb{CT}}(\mathcal{T}_S^D, \lvert\mathfrak{M}_T\rvert^2, T)$ (s^{-1})					
	CV/CdS system			CV/InAs system		
	1-propanol 0.611811	Acetonitrile 0.686607	Ethanol 0.646761	1-propanol 0.5437945	Acetonitrile 0.616523	Ethanol 0.577585
0.020	5.05228×10^{-37}	5.2121×10^{-37}	5.3695×10^{-37}	3.7146×10^{-39}	3.4898×10^{-39}	3.6049×10^{-39}
0.022	6.07513×10^{-37}	5.7333×10^{-37}	5.9065×10^{-37}	4.0861×10^{-39}	3.8388×10^{-39}	3.9654×10^{-39}
0.024	6.6271×10^{-37}	6.2545×10^{-37}	6.4434×10^{-37}	4.4576×10^{-39}	4.1878×10^{-39}	4.3251×10^{-39}
0.026	7.1797×10^{-37}	6.7757×10^{-37}	6.9804×10^{-37}	4.8290×10^{-39}	4.5368×10^{-39}	4.6864×10^{-39}
0.028	7.7319×10^{-37}	7.2971×10^{-37}	7.5173×10^{-37}	5.2005×10^{-39}	4.8850×10^{-39}	5.0469×10^{-39}
0.030	8.2841×10^{-37}	7.8182×10^{-37}	8.0543×10^{-37}	5.072×10^{-39}	5.2348×10^{-39}	5.0469×10^{-39}

Table 7. The charge flow rate of electron transfer $\Lambda_{\mathbb{CT}}(\mathcal{T}_S^D, |\mathfrak{M}_T|^2, T)$.

Average coupling coefficient	The charge flow rate of electron transfer $\Lambda_{\mathbb{CT}}(\mathcal{T}_S^D, \lvert\mathfrak{M}_T\rvert^2, T)$ (s^{-1})					
	N3/CdS system			N3/InAs system		
	1-propanol 0.387112	Acetonitrile 0.434637	Ethanol 0.409217	1-propanol 0.3398633	Acetonitrile 0.385951	Ethanol 0.361161
0.020	6.9292×10^{-37}	6.5423×10^{-37}	6.7409×10^{-37}	4.6922×10^{-39}	4.4041×10^{-39}	4.5515×10^{-39}
0.022	7.6221×10^{-37}	7.1965×10^{-37}	7.4150×10^{-37}	5.1614×10^{-39}	4.8445×10^{-39}	5.0066×10^{-39}
0.024	8.3150×10^{-37}	7.8507×10^{-37}	8.0891×10^{-37}	5.6307×10^{-39}	5.2849×10^{-39}	5.4618×10^{-39}
0.026	9.0080×10^{-37}	8.8050×10^{-37}	8.7632×10^{-37}	6.0999×10^{-39}	5.7253×10^{-39}	5.9169×10^{-39}
0.028	9.7009×10^{-37}	9.159×10^{-37}	9.437×10^{-37}	6.51691×10^{-39}	6.1659×10^{-39}	6.3721×10^{-39}
0.030	1.0393×10^{-36}	9.8134×10^{-37}	1.0111×10^{-36}	7.0383×10^{-39}	6.6062×10^{-39}	6.8272×10^{-39}

depth refer to the medium region of electronic transition reaction. However, the transition of electrons depends on the electron driving energy (the required energy for electrons to transfer over a potential of material interfaces), and this driving energy supplied to a system by absorption of the dye in both systems as shown in Fig. 2. This energy facilitates the electrons injection results in from more electrons transfer from donor states to acceptor states across the interface of the conduction state to dye states in N3 and CV dyes as seen in Tables 3 and 4 It is clear from Tables 3 and 4 that the electron driving energies for N3/CdS and N3/InAs systems are higher than that in the Cv/CdS and CV/InAs systems, and these high energies lead to increase the flow charge rate for N3/CdS and N3/InAs compared to Cv/CdS and CV/InAs as shown in Tables 6 and 7.

In the interface of DSSC, the potential barrier depends on the structure of material and indicates the characteristics of the energy levels at the Highest Occupied Molecular Orbital (HOMO) and the Lowest Unoccupied Molecular Orbital (LUMO) for N3 and CV, and the energy levels in the conduction band for CdS and InAs semiconductors. According to the results of energy of transition in four systems that shown in Tables 2 and 3, it is clear that the N3/CdS and N3/InAs systems need lower energy to reconfigure and transfer than that for CV/CdS and CV/InAs systems. Therefore, a system with lower transferring energy has higher charge flow rate and vice versa for all the three solvents. Tables 2 and 3 show that the energy transfer of electrons in both systems with Acetontrile solvent is higher than those with the 1-propanol and Ethanol solvents. Tables 6 and 7 show that N3/CdS and N3/InAs systems have higher flow charge transfer than CV/CdS and CV/InAs systems, this indicates that N3/CdS and N3/InAs systems have lower potential barriers than other systems. From the results in Tables 6 and 7, the systems with 1-Propanol and Ethanol solvents have faster formation to transition than those of Acetontrile solvents along with larger flow charge transition through the interface. Also, 1-Propanol solvent was the most active media to transfer than other solvents. The Acetonitrile solvent in all systems results in more transition energy to reform to transfer and low flow charge for the transfer. On the other hand, a comparison of the regional media for charge transfer as a function of the polarity for both systems with three solvents shows that the flow charge rate increases with increasing the polarity and leads to increasing the DSSC efficiency. Tables 6 and 7 show that the flow charge rate of N3/CdS and CV/CdS systems is faster than that for N3/InAs and CV/ InAs systems, which confirms that CdS is

the most active semiconductor for N3 and CV dye systems. Furthermore, the results in Tables 6 and 7 also shows that the charge flow rate for all systems increases with increasing the coupling.

5. Conclusions

In this study, a comprehensive the scenario dynamic of charge transfer and calculations the efficiency with electronic properties of DSSC systems as function of flow charge rate was carried out.

The flow charge rate of N3/CdS, N3/InAs, CV/CdS and CV/InAs was proportional increase with decreasing the energy of transition and increasing the coupling parameter. The flow charge rate is effected by potential at the interface in DSSC devices, it increases with decreases the potential height and vice versa. The flow charge rate at DSSC system is active with propanol compared with other solvent, it is the most active polar solvent to charge transfer compared to other solvents. The results of the flow charge rate indicate that CdS was the most active alignment system for N3 and CV dyes for electronic transfer reaction

References

[1] O. Edenhofer, P.M. Ramón, S. Youba, in: C.V. Stechow (Ed.), IPCC special report on renewable energy sources and climate change mitigation, Cambridge University Press, Cambridge, 2011, p. 167.
[2] F.V. Molefe, M. Khenfouch, M.S. Dhlamini, B.M. Mothudi, Spectroscopic investigation of charge and energy transfer in P3HT/GO nanocomposite for solar cell applications, Adv Mater Lett 8 (3) (2017) 246–250.
[3] J.G. Canadell, C. Le Quéré, M.R. Raupach, C.B. Field, E.T. Buitenhuis, P. Ciais, T.J. Conway, N.P. Gillett, R.A. Houghton, G. Marland, Contributions to accelerating atmospheric CO2 growth from economic activity, carbon intensity, and efficiency of natural sinks, Proc Natl Acad Sci 104 (47) (2007) 18866–18870.
[4] Würfel, Physics of solar cells: From basic principles to advanced concepts, John Wiley & Sons, 2009.
[5] T. Dittrich, Materials concepts for solar cells (Vol. 1), World Scientific Publishing Company, 2014.
[6] A.A. Al-Khafaji, D.B. Alwan, F.H. Ali, W.A. Twej, Influence of grain size, electrode type and additives on dye sensitized solar cells efficiency, Environ Sci Indian J 12 (6) (2016) 217–223.
[7] O.V. Prezhdo, W.R. Duncan, V.V. Prezhdo, Dynamics of the photoexcited electron at the chromophore–semiconductor interface, Accounts Chem Res 41 (2) (2008) 339–348.
[8] C. Cavallo, F. Di Pascasio, A. Latini, M. Bonomo, D. Dini, Nanostructured semiconductor materials for dye-sensitized solar cells, J Nanomater (2017).
[9] R.L. Carroll, C.B. Gorman, The genesis of molecular electronics, Angew Chem Int Ed 41 (23) (2002) 4378–4400.
[10] H.J.M. Al-Agealy, R.I.N. AL-Obaidi, Electron transfer at semiconductor/liquid. interfaces, Ibn AL-Haitham J Pure Appl Sci 22 (2) (2009).
[11] Y.Q. Gao, R.A. Marcus, On the theory of electron transfer reactions at semiconductor/liquid interfaces, II. A free electron model, J Chem Phys 113 (15) (2000) 6351–6360.
[12] M. Andrea, Marcus theory for electron transfer a short introduction, MPIP J Club-Mainz (2008).
[13] S.G. Shachi, Electron transfer at metal surfaces (Doctoral dissertation, Ph. D, theses), California Institute of TechnologyPasadena, California, 2002.
[14] Y.Q. Gao, Y. Georgievskii, R.A. Marcus, On the theory of electron transfer reactions at semiconductor electrode/liquid interfaces, J Chem Phys 112 (7) (2000) 3358–3369.
[15] C. Creutz, B.S. Brunschwig, N. Sutin, Interfacial charge-transfer absorption: 3. application to semiconductor- molecule assemblies, J Phys Chem B 110 (50) (2006) 25181–25190.
[16] H.J. Al-agealy, B. Alshafaay, M.A. Hassooni, A.M. Ashwiekh, A.K. Sadoon, R.H. Majeed, R.Q. Ghadhban, S.H. Mahdi, Theoretical discussion of electron transport rate constant at TCNQ/Ge and TiO2 system, J Phys Conf Ser 1003 (1) (2018) 012122, IOP Publishing.
[17] S.M. Sze, Physics of semiconductor devices, 2nd ed., John Wiley & Sons, 1981.
[18] D.R. Lide, CRC handbook of chemistry and physics, Google Scholar, Chemical Rubber, Boca Raton, FL, 1998, pp. 10–198.
[19] P. Patnaik, Handbook of inorganic chemicals, McGraw-Hill, New York, 2003.